Korean J. Chem. Eng., **26**(1), 115-126 (2009)

Gene expression profiling in streptozotocin-induced diabetic rat liver in response to fungal polysaccharide treatment

Hye Jin Hwang, Sang Woo Kim, Yu Mi Baek, Sung Hak Lee, Hee Sun Hwang, and Jong Won Yun†

Department of Biotechnology, Daegu University, Gyeongsan, Gyeongbuk 712-714, Korea
(*Received 22 April 2008 • accepted 22 June 2008*)

Abstract−We established the gene expression profiling in streptozotocin (STZ)-induced diabetic rat liver in response to hypoglycemic fungal polysaccharides (EPS), using oligonucleotide microarray analysis. Differentially regulated genes showing higher fold change than 2 were identified and categorized through hierarchical clustering analysis. Among the 835 genes analyzed, 244 were up-regulated, while 321 were down-regulated after diabetes induction. Interestingly, many gene expressions altered after STZ-treatment mimicked a normal rat liver by EPS therapy. Most of these genes included genes involving cell structure and motility, immunity and defense, lipid, fatty acid and steroid metabolism, protein metabolism and modification, and signal transduction. More importantly, we found a total of 36 genes that showed significant fold changes in their expression that have not previously been examined in the context of diabetes. To validate the microarray results, we further confirmed the gene expression patterns by RT-PCR using four genes of interest (carboxylesterase 2, stearoyl-coenzyme A desaturase 1, insulin-like growth factor 1, and insulin-like growth factor binding protein 2). Taken together, EPS acted as a potent regulator of gene expression for a wide variety of genes in diabetic rat liver.

Key words: Diabetes Mellitus, Fungal Polysaccharides, Gene Profile, Microarray, Streptozotocin

INTRODUCTION

Diabetes is associated with significant morbidity and mortality, and is a contributor to the development of other diseases. For example, the onset of diabetes is accompanied by development of major biochemical and functional abnormalities especially in the liver, including alterations in carbohydrate, lipid, and protein metabolism, and changes in antioxidant status [1-6]. These abnormalities are particularly important because of their impact on the systemic effects of liver function, especially maintenance of blood glucose homeostasis. Since insulin cannot be used orally and continuous use of the synthetic antidiabetic drugs causes side effects and toxicity [7,8], a variety of oral hypoglycemic agents are available for the treatment of diabetes mellitus, by increasing demand by patients to use natural products with antidiabetic activity [9-12].

In our previous study [13], it was found that fungal polysaccharides produced from mycelial culture of a medicinal mushroom *Phellinus baumii* had a strong antidiabetic activity. More recently, we obtained interesting results using those polysaccharides that plasma proteome was significantly altered in STZ-induced diabetic rats in response to polysaccharide therapy [14,15].

A recent advancement in genomic research, microarray technology, allows for the expression of thousands of genes to be quickly and easily monitored in parallel [16-18]. Global gene expression, or transcriptional profiling, has been used to identify molecular markers for various pathological states, and can be used to generate novel hypotheses to characterize different disease states [19-23]. DNA microarrays have been used to identify candidate genes for disease diagnosis, and to characterize gene expression patterns associated with potential disease treatments including diabetes [24-26]. However, the genetic changes involved in the pathology of diabetes have not been fully identified so far [27]. Several reports have focused on the molecular genetic effects associated with STZ-induced diabetes [28-30]. However, there is still a lack of knowledge about the changes in gene expression in STZ-induced diabetic animals before and after treatments of anti-diabetic drugs or other candidate materials.

To make track for the molecular action and mechanism of the hypoglycemic fungal polysaccharides responsible for STZ-induced diabetes through the regulation of the liver function, the present study was designed to examine the gene expression profiling in isolated rat liver treated with fungal polysaccharide using an oligonucleotide microarray.

MATERIALS AND METHODS

1. Preparation of the Exopolysaccharides (EPS)

The EPS was prepared as described previously [13]. Briefly, the submerged culture of *P. baumii* for the preparation of EPS was performed in a 5-*l* stirred-tank fermenter under the defined culture conditions. The resulting culture filtrate was mixed with four volumes of absolute ethanol, stirred vigorously, and left overnight at 4 °C. The precipitated EPS was harvested by centrifugation at 10,000 ×*g* for 20 min, lyophilized, and used for animal experiments without further purification. The carbohydrate and protein contents in the crude EPS were 71.0% and 29.0%, respectively. The crude EPS consisted of mainly arginine (14.1%) and glycine (12.0%) in protein moiety and mainly mannose (48.7%) and arabinose (38.4%) in carbohydrate moiety (data not shown).

2. Animal Experiments

Male Sprague-Dawley rats (Daehan Experimental Animals, Seoul, Korea) weighing 130-150 g at 5 weeks of age were bred as described

†To whom correspondence should be addressed.
E-mail: jwyun@daegu.ac.kr

previously [13-15]. In brief, diabetes was induced by intravenous injection of streptozotocin (50 mg/kg body weight, dissolved in 0.01 M sodium citrate buffer, pH 4.5). Control rats were injected with vehicle alone. Diabetes was verified 48 h later by evaluating blood glucose levels with the use of glucose oxidase reagent strips (Lifescan, Milpitas, CA, USA). Rats with a blood glucose level ≥300 mg/dl (16.7 mmol/*l*) were considered to be diabetic. All the animals were randomly divided into three groups with six animals in each group: normal healthy control group (N group), normal rats received 0.9% NaCl solution; STZ-induced diabetic group (STZ group), diabetic rats treated with 0.9% NaCl solution; EPS-treated diabetic group (EPS group), diabetic rats treated with EPS at the level of 200 mg/kg body weight daily for 14 days. The EPS-fed control group was excluded in this study because of similar physiological status to normal control group as described in our previous studies [14,15]. These experiments were approved by the Committee for Laboratory Animal Care and Use, Daegu University. All procedures were conducted in accordance with the "Guide for the Care and Use of Laboratory Animals" published by the National Institutes of Health.

3. Isolation of Total RNA

Total RNA from frozen tissue was isolated with the RNeasy Mini Kit (Qiagen, Stanford, CA). Tissue was resuspended in buffer RLT (RNeasy Lysis Buffer) and homogenized by passing the lysate five times through a 23-gauge needle fitted to a syringe. The samples were then processed following the manufacturer's instructions. In the final step, the RNA was eluted with 50 μl of RNase-free water by centrifugation for 1 min at 10,000 rpm. Quality of the RNA was analyzed on a 1% agarose gel and the concentration by an RNA/DNA spectrophotometer (Spectronic Instruments, Rochester, NY).

4. Microarray Analysis

Applied Biosystems 1700 Full Genome Expression Rat Microarray was used to analyze the transcriptional profiles of three tissues RNA samples (normal, STZ-treated and EPS-treated tissues). The microarray includes 26,857 probe designs against 27,088 genes that cover 43,508 transcripts.

Digoxigenin-UTP labeled cRNA was generated and linearly amplified from 1 μg of total RNA using Applied Biosystems Chemiluminescent RT-IVT Labeling Kit and manufacturer's protocol (Applied Biosystems, Foster City, CA). Array hybridization (two arrays per sample), chemiluminescence detection, image acquisition and analysis were performed using Applied Biosystems Chemiluminescence Detection Kit and Applied Biosystems 1700 Chemiluminescent Microarray Analyzer following the manufacturer's protocol. Briefly, each microarray was first prehybridized at 55 °C for 1 hr in hybridization buffer with blocking reagent. 10 μg of labeled cRNA targets was first fragmented into 100-400 bases by incubating with fragmentation buffer at 60 °C for 30 min, mixed with internal control target (ICT, 24-mer oligo labeled with LIZ® fluorescent dye) and hybridized to each pre-hybrid microarray in a 0.5 ml volume at 55 °C for 16 hr. After hybridization, the arrays were washed with hybridization wash buffer and chemiluminescence rinse buffer. Enhanced chemiluminescent signals were generated by first incubating arrays with anti-digoxigenin-alkaline phosphatase, enhanced with chemiluminescence enhancing solution and finally adding chemiluminescence substrate. Eight images were collected for each microarray by using the 1700 analyzer which is equipped with high-resolution, large-format CCD camera, including two "short" chemiluminescent images (5 seconds exposure length each) and two "long" chemiluminescent images (25 seconds exposure length each) for gene expression analysis, two fluorescent images for feature finding and spot normalization and two QC images for spectrum cross-talk correction. Images were auto-gridded and the chemiluminescent signals were quantified, corrected for background and spot and spatially normalized.

Table 1. Primer sequences used for RT-PCR

Gene symbol	Primer sequence
β-actin	forward 5'-AGCCATGTACGTAGCCATCC-3'
	reverse 5'-CTCTCAGCTGTGGTGGTGAA-3'
Ces2	forward 5'-CAAGAGTGGAGCAGAGATTC-3'
	reverse 5'-ATTTGTGCTGCTGTATCCTT-3'
Scd1	forward 5'-AACGATGTATATGAATGGGC-3'
	reverse 5'-TACCTCCTCTGGAACATCAC-3'
Igf1	forward 5'-CTGGGTGTCCAAATGTAACT-3'
	reverse 5'-GTATCTTTATTGGAGGTGCG-3'
Igfbp2	forward 5'-GAAAGAGACCAACACTGAGC-3'
	reverse 5'-GACACAGGGGTTCAAAAATA-3'

5. Image Analysis

Scans were performed on the Applied Biosystems 1700 Chemiluminescent Microarray Analyzer version 1.1.0 (http://www.appliedbiosystems.com). Differences in microarray intensities were normalized and grouped by using the Avadis Prophetic 3.3 version (Strand Genomics Pvt. Ltd., (http://avadis.strandgenomics.com)).

6. Reverse Transcriptase PCR (RT-PCR)

RT-PCR was performed by using the One Step RT-PCR kit (Qiagen, Valencia, CA) with gene specific primers as shown in Table 1. PCR reactions were performed in a thermal cycler (Techne, Princeton, NJ, USA) under the following conditions: 50 °C for 30 min, 95 °C for 15 min (1 cycle); 94 °C for 30 sec, 50 °C for 30 sec, and 72 °C for 1 min (30 cycles). PCR products were electrophoresed on 1% agarose gel containing ethidium bromide (0.5 μg/ml) and were visualized as a single compact band of expected size under UV light and documented by gel documentation system.

RESULTS AND DISCUSSION

There has been little evidence that natural compounds themselves directly modulate the liver gene expression. Hence, we examined the gene expression profile of rat liver treated with anti-diabetic polysaccharides and the potency of a hypoglycemic function of fungal polysaccharides in liver through the DNA microarray analysis.

We compared the gene expression profile of liver tissue from control, STZ- and EPS-treated rats on day 14. It was found that the rat liver treated with STZ caused many changes in the gene expression. Among the total of 835 genes analyzed, 565 genes, showing more than two-fold differences in response to STZ treatment, were counted as differentially expressed genes in rat liver. In this study, PANTHER classification system (http://www.pantherdb.org) was used to classify genes according to their functions [31]. Briefly, gene lists (e.g., from mRNA expression data) can be uploaded to the site and analyzed relative to molecular functions, biological processes and pathways. Fig. 1 shows the functional classification of

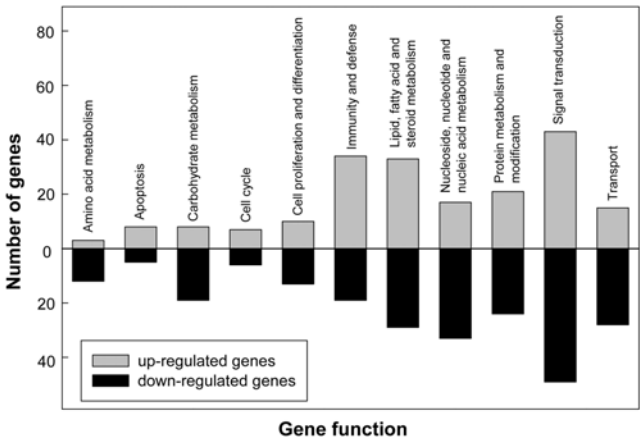

Fig. 1. Functional classification of differentially expressed genes in STZ-induced diabetic rat liver.

differentially expressed genes in STZ-induced diabetic rat liver. It is interesting to mention that STZ down-regulated many genes involved in carbohydrate and amino acid metabolism, whereas up-regulated more genes involved in immunity and defense, lipid, fatty acid and steroid metabolism, and signal transduction (Fig. 1).

Hierarchical clustering was used to aid visualization and biological interpretation of this extensive data set, and in particular, to identify correlated expression patterns that reflect potential biological/toxicological processes occurring in the liver tissues of the rats treated with STZ and EPS. Fig. 2A shows the hierarchical clustering display of data for the rat liver of the three experimental groups based on the 835 filtered genes. Each gene is represented by a single row of colored bars. The 835 genes were grouped into nine clusters each containing 32-257 genes. Fig. 2B shows the profiles of the clustering (up-regulated, down-regulated, and not changed compared to the normal group after STZ treatments). Interestingly, the profiles of clusters 1, 2, 3, 4, 5, 8, and 9 (totally 716 genes) showed significant difference between the normal and diabetic rat liver in response to STZ and EPS treatments. The clusters 2, 3, 4, and 9 were up-regulated genes by STZ treatment and got back to around normal expression levels by EPS therapy. Most of these up-regulated genes included genes involved in immunity and defense, lipid, fatty acid and steroid metabolism, nucleoside, nucleotide and nucleic acid metabolism, protein metabolism and modification, and signal transduction. The clusters 1, 5, and 8 were down-regulated genes by STZ treatment and returned approximately to normal levels by EPS treatment. Most of these down-regulated genes included genes involved in carbohydrate metabolism, lipid, fatty acid and steroid metabolism, nucleoside, nucleotide and nucleic acid metabolism, protein metabolism and modification, signal transduction, and transport. It is obvious that EPS therapy played a pivotal role in normal gene regulation in diabetic rat liver that was dysregulated by STZ. Unlike others, genes of cluster 6 and 7 showed no difference in response to EPS treatments, which could not be clarified in this study.

Table 2 shows the list of the up- and down-regulated genes between STZ- and EPS-treated diabetic rats (fold change>2). The up- or down-regulated genes were categorized by their functions.

1. Amino Acid Metabolism

Abnormal amino acid metabolism is sometimes observed among patients with diabetes mellitus [32]. About 80% of genes in amino acid metabolism were down-regulated including argininosuccinate lyase, carnitine O-octanoyltransferase, cysteine-sulfinate decarboxylase, glutamate oxaloacetate transaminase 1, 3-phosphoglycerate dehydrogenase, and tyrosine aminotransferase (Table 2 and Fig. 1). These expression changes might be related to the abnormal amino acid metabolisms mediated by STZ, where the expression levels of

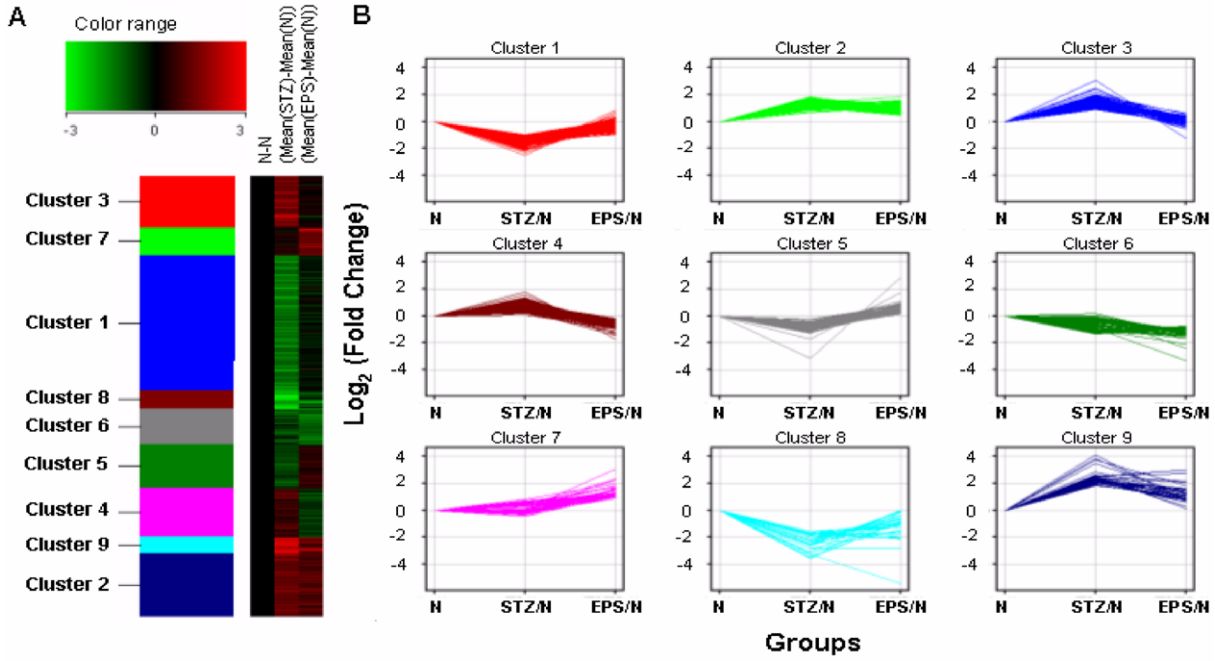

Fig. 2. Gene expression profiles of diabetic rat liver. A: Hierarchical clustering of data based on the 10,290 filtered genes, B: the expression patterns of genes in each cluster.

Table 2. Genes up- or down-regulated by STZ induced diabetes in rat liver[a]

Gene ID	Gene name	Fold (STZ/N)[b]	Fold (EPS/N)[b]	Cluster
Amino acid metabolism				
rCG33563	amine oxidase, copper containing 2 (retina-specific)	1.225	2.162	7
rCG21476	argininosuccinate lyase	−2.052	−1.540	1
rCG41076	carnitine O-octanoyltransferase	−5.443	−1.970	8
rCG50590	cysteine sulfinic acid decarboxylase	−8.595	1.039	8
rCG24456	dopa decarboxylase	−2.427	−1.288	1
rCG33632	fatty acid synthase	4.676	3.054	9
rCG51181	glycine cleavage system protein H (aminomethyl carrier)	−2.125	−1.066	1
rCG57649	glutamate oxaloacetate transaminase 1	−3.562	−1.807	8
rCG37702	kynureninase (L-kynurenine hydrolase)	−2.823	−1.328	1
rCG51978	3-phosphoglycerate dehydrogenase	−1.901	−3.166	6
rCG21299	serine dehydratase	−4.919	−1.509	8
rCG26600	solute carrier family 1 (glial high affinity glutamate transporter), member 2	2.133	−1.288	4
rCG51300	tyrosine aminotransferase	−2.582	−1.211	1
Apoptosis				
rCG49353	adenomatosis polyposis coli	1.668	−1.429	4
rCG53149	baculoviral IAP repeat-containing 4	−2.139	−1.451	1
rCG31859	caspase 12	1.530	−1.404	4
rCG62399	EGL nine homolog 3 (*C. elegans*)	2.393	1.551	2
rCG44446	granzyme K	3.553	2.181	9
rCG41634	interleukin 7	1.274	2.760	7
rCG60290	lectin, galactose binding, soluble 1	−2.213	−1.534	1
rCG36262	melanoma antigen, family D, 1	−2.047	−1.303	1
rCG54388	peptidoglycan recognition protein 1	2.127	1.938	2
rCG35087	suppressor of cytokine signaling 3	4.140	1.838	9
Carbohydrate metabolism				
rCG28864	alcohol dehydrogenase 7 (class IV), mu or sigma polypeptide	1.513	2.188	7
rCG49423	UDP-Gal:betaGlcNAc beta 1,4-galactosyltransferase, polypeptide 6	2.069	1.638	2
rCG23512	crystallin, lamda 1	3.750	1.254	3
rCG33892	dodecenoyl-coenzyme A delta isomerase	−2.924	−1.321	1
rCG53633	enoyl coenzyme A hydratase 1, peroxisomal	−2.047	1.017	1
rCG44062.1	HNF-3/forkhead homolog-1	5.272	1.541	9
rCG34259	glucose-6-phosphatase, catalytic	−2.126	−1.009	1
rCG55118	glucosamine (UDP-N-acetyl)-2-epimerase/N-acetylmannosamine kinase	−1.724	1.308	5
rCG36418	glycerol kinase	−3.201	−1.328	1
rCG51841.1	hydroxyacid oxidase 2 (long chain)	−1.795	1.133	5
rCG53940	lactate dehydrogenase A	−3.416	−1.310	1
rCG31944	leukotriene B4 12-hydroxydehydrogenase	−2.333	1.034	1
rCG23753	neuraminidase 2	5.567	1.236	9
rCG54388	peptidoglycan recognition protein 1	2.127	1.938	2
rCG60289.1	peroxisome proliferator activated receptor alpha	−2.829	−1.641	1
rCG50988	protein kinase, AMP-activated, alpha 1 catalytic subunit	2.329	2.830	2
rCG55421	UDP-glucuronosyltransferase	5.044	4.200	9
rCG21299	serine dehydratase	−4.919	−1.509	8
rCG30703.1	solute carrier family 2, member 5	−1.266	2.856	7
Cell cycle				
rCG22805	septin 7	−2.134	−1.247	1
rCG49353	adenomatosis polyposis coli	1.668	−1.429	4
rCG46238	B-cell translocation gene 2, anti-proliferative	2.512	1.469	2
rCG48202	cyclin D1	−1.239	−2.096	6
rCG60712.1	cell division cycle 2 homolog A (*S. pombe*)	2.083	−1.165	3

Table 2. Continued

Gene ID	Gene name	Fold (STZ/N)[b]	Fold (EPS/N)[b]	Cluster
rCG44062.1	HNF-3/forkhead homolog-1	5.272	1.541	9
rCG53510.1	v-jun sarcoma virus 17 oncogene homolog (avian)	3.328	1.106	3
rCG34431	lethal giant larvae homolog 1 (Drosophila)	1.412	−1.695	4
rCG44964.1	ribosomal protein S6 kinase polypeptide 2	1.274	−1.851	4
Cell proliferation and differentiation				
rCG46238	B-cell translocation gene 2, anti-proliferative	2.512	1.469	2
rCG48202	cyclin D1	−1.239	−2.096	6
rCG55777	core promoter element binding protein	1.499	−1.401	4
rCG60405	chemokine (C-X-C motif) ligand 1	7.167	2.510	9
rCG49298	diphtheria toxin receptor	1.864	−1.935	4
rCG48966	dual specificity phosphatase 6	1.885	−1.507	4
rCG28070	Eph receptor B6 (predicted)	−1.696	1.414	5
rCG44604.1	endothelial cell-specific molecule 1	−2.018	1.987	5
rCG54320.1	fibroblast growth factor 21	−3.413	−2.176	8
rCG44062.1	HNF-3/forkhead homolog-1	5.272	1.541	9
rCG48929	insulin-like growth factor 1	−2.830	−1.158	1
rCG60295.1	inhibin beta C	−2.949	−1.265	1
rCG59891	inhibin beta E	−3.496	1.129	1
rCG53510.1	v-jun sarcoma virus 17 oncogene homolog (avian)	3.328	1.106	3
rCG30255	Kirsten rat sarcoma viral oncogene homologue 2 (active)	−1.183	1.723	5
rCG47320	multiple inositol polyphosphate histidine phosphatase 1	−2.952	−1.386	1
rCG46454	myogenin	−3.444	1.010	1
rCG43164	neuregulin 1	3.952	1.189	3
rCG60289.1	peroxisome proliferator activated receptor alpha	−2.829	−1.641	1
rCG61648.1	protein kinase C, epsilon	1.313	−1.956	4
rCG28308	pleiotrophin	−3.353	−2.079	8
rCG59982	somatostatin receptor 3	2.427	2.856	2
rCG61469.1	twist gene homolog 1 (Drosophila)	−1.007	2.001	7
Immunity and defense				
rCG29689	alpha-2-macroglobulin	−3.486	1.283	1
rCG34752	arachidonate 12-lipoxygenase	−1.267	−2.617	6
rCG37559	angiopoietin-like protein 4	−1.998	1.662	5
rCG33563	amine oxidase, copper containing 2 (retina-specific)	1.225	2.162	7
rCG51010	complement component 6	−1.671	1.930	5
rCG34044	chemokine (C-C motif) ligand 3	1.821	−1.287	4
rCG44286	carboxylesterase 1	1.684	−1.515	4
rCG57590	carboxylesterase 2	3.112	−1.060	3
rCG39038	carboxylesterase 5	1.983	−1.280	4
rCG39026	carboxylesterase 6	1.345	−1.747	4
rCG55777	core promoter element binding protein	1.499	−1.401	4
rCG20212	complement receptor related protein	−2.340	−1.087	1
rCG46116.1	cathepsin E	−2.167	−1.805	6
rCG58730	coxsackie virus and adenovirus receptor	1.355	−2.458	4
rCG60405	chemokine (C-X-C motif) ligand 1	7.167	2.510	9
rCG52144	epoxide hydrolase 2, cytoplasmic	−2.029	−1.199	1
rCG46303	Fc receptor, IgG, low affinity IIb	2.155	1.166	3
rCG44446	granzyme K	3.553	2.181	9
rCG21815	heat shock 27 kDa protein 1	4.727	2.081	9
rCG27617	immunoglobulin heavy chain (alpha polypeptide)	−6.998	−7.015	8
rCG41634	interleukin 7	1.274	2.760	7
rCG50886.1	integrin beta 1	1.134	2.422	7

Table 2. Continued

Gene ID	Gene name	Fold (STZ/N)[b]	Fold (EPS/N)[b]	Cluster
rCG30109	killer cell lectin-like receptor, subfamily D, member 1	2.104	1.637	2
rCG60290	lectin, galactose binding, soluble 1	−2.213	−1.534	1
rCG39425	NADPH oxidase 4	−3.493	−1.222	1
rCG21913	2',5'-oligoadenylate synthetase 1, 40/46 kDa	1.870	−1.194	4
rCG55185	orosomucoid 1	2.040	2.697	2
rCG54388	peptidoglycan recognition protein 1	2.127	1.938	2
rCG60289.1	peroxisome proliferator activated receptor alpha	−2.829	−1.641	1
rCG49547	protein phosphatase 2 (formerly 2A), regulatory subunit B (PR 52), beta isoform	2.448	1.757	2
rCG50988	protein kinase, AMP-activated, alpha 1 catalytic subunit	2.329	2.830	2
rCG62602	S100 calcium binding protein A8 (calgranulin A)	2.770	2.334	2
rCG62481	S100 calcium binding protein A9 (calgranulin B)	1.968	2.044	2
rCG20360	serum amyloid P-component	−2.155	−1.033	1
Lipid, fatty acid and steroid metabolism				
rCG35202	acyl-Coenzyme A dehydrogenase, very long chain	−1.624	−2.141	6
rCG34752	arachidonate 12-lipoxygenase	−1.267	−2.617	6
rCG23669	alpha-methylacyl-CoA racemase	−2.996	−1.234	1
rCG47519	annexin A1	−2.291	−1.844	6
rCG58473	apolipoprotein A-IV	−3.046	−1.035	1
rCG58386	apolipoprotein A-V	−2.004	−1.423	1
rCG28162	caveolin 2	−4.809	−1.273	8
rCG28162	caveolin 2	−4.395	−1.442	8
rCG41076	carnitine O-octanoyltransferase	−5.443	−1.970	8
rCG23512	crystallin, lamda 1	3.750	1.254	3
rCG57693	cytochrome P450, family 17, subfamily a, polypeptide 1	−9.199	−1.734	8
rCG57447	cytochrome P450, family 2, subfamily c, polypeptide 40	−1.745	−2.012	6
rCG57514	cytochrome P450, family 2, subfamily c, polypeptide 70	3.147	1.139	3
rCG55954	cytochrome P450, family 3, subfamily a, polypeptide 13	5.069	1.503	9
rCG41001	cytochrome P450, subfamily 51	1.915	2.016	2
rCG30398.1	cytochrome P450, family 7, subfamily a, polypeptide 1	2.187	1.117	3
rCG41340	cytochrome P450, family 7, subfamily b, polypeptide 1	5.335	−1.254	3
rCG25275	cytochrome P450, family 8, subfamily b, polypeptide 1	−5.730	1.002	8
rCG33892	dodecenoyl-coenzyme A delta isomerase	−2.924	−1.321	1
rCG47183	7-dehydrocholesterol reductase	2.020	1.476	2
rCG53633	enoyl coenzyme A hydratase 1, peroxisomal	−2.047	1.017	1
rCG28808	fatty acid binding protein 2, intestinal	−1.613	−2.066	6
rCG21961	fatty acid binding protein 7, brain	−3.342	−2.079	8
rCG33632	fatty acid synthase	4.676	3.054	9
rCG52241.1	farnesyl diphosphate farnesyl transferase 1	2.018	1.612	2
rCG50915.1	glyceronephosphate O-acyltransferase	−2.009	−1.084	1
rCG57756	glycerol-3-phosphate acyltransferase, mitochondrial	1.598	−1.496	4
rCG44692	3-hydroxy-3-methylglutaryl-Coenzyme A reductase	5.594	2.623	9
rCG44679	3-hydroxy-3-methylglutaryl-Coenzyme A synthase 1	2.314	2.553	2
rCG51973	3-hydroxy-3-methylglutaryl-Coenzyme A synthase 2	−2.107	1.068	1
rCG56782	insulin induced gene 1	2.814	1.758	2
rCG20089	lamin B receptor	1.040	−2.260	6
rCG23753	neuraminidase 2	5.567	1.236	9
rCG40128	olfactory specific medium-chain acyl CoA synthetase	−1.956	1.030	1
rCG53524.1	ER transmembrane protein Dri 42	−2.720	−1.234	1
rCG60289.1	peroxisome proliferator activated receptor alpha	−2.829	−1.641	1
rCG21954	prosaposin	−2.455	−1.057	1
rCG60176	retinol dehydrogenase 2	−2.131	−1.218	1

Table 2. Continued

Gene ID	Gene name	Fold (STZ/N)[b]	Fold (EPS/N)[b]	Cluster
rCG48482	cytochrome P450, family 26, subfamily A, polypeptide 1	13.359	3.571	9
rCG52982	phosphatidylserine-specific phospholipase A1	2.835	−1.087	3
rCG29433	cytochrome P450 4F5	1.308	−1.761	4
rCG39286	kidney-specific protein (KS)	5.516	1.936	9
rCG55421	UDP-glucuronosyltransferase	5.044	4.200	9
rCG39362	SA rat hypertension-associated homolog	2.383	1.870	2
rCG54684	sterol-C4-methyl oxidase-like	2.525	2.716	2
rCG57790	stearoyl-Coenzyme A desaturase 1	−8.719	7.101	5
rCG53385	sulfotransferase family, cytosolic, 1C, member 2	−2.210	−2.258	6
rCG53385	sulfotransferase family, cytosolic, 1C, member 2	−2.130	−2.609	6
Nucleoside, nucleotide and nucleic acid metabolism				
rCG55777	core promoter element binding protein	1.499	−1.401	4
rCG45317	cAMP responsive element modulator	−2.234	−1.341	1
rCG49327	early growth response 1	2.436	−2.596	4
rCG35497	elaC homolog 2 (*E. coli*)	−2.001	−1.072	1
rCG37183	E74-like factor 1	2.019	1.177	3
rCG44062.1	HNF-3/forkhead homolog-1	5.272	1.541	9
rCG55118	glucosamine (UDP-N-acetyl)-2-epimerase/N-acetylmannosamine kinase	−1.724	1.308	5
rCG42352.1	guanine nucleotide binding protein-like 3 (nucleolar)	1.992	2.686	2
rCG62549	guanylate cyclase 1, soluble, alpha 3	−2.189	−1.170	1
rCG57472	guanylate cyclase 2 g	−2.720	−1.166	1
rCG36641	hairy and enhancer of split 1 (Drosophila)	−2.012	−1.767	6
rCG45142	germinal histone H4 gene	3.146	−1.443	3
rCG30869	Inhibitor of DNA binding 3, dominant negative helix-loop-helix protein	2.001	−1.328	4
rCG53510.1	v-jun sarcoma virus 17 oncogene homolog (avian)	3.328	1.106	3
rCG46454	myogenin	−3.444	1.010	1
rCG33586	neurogenic differentiation 2	2.251	1.231	3
rCG21913	2',5'-oligoadenylate synthetase 1, 40/46 kDa	1.870	−1.194	4
rCG25272	one cut domain, family member 1	−5.901	−1.488	8
rCG53397	phosphodiesterase 4B	−2.520	−1.952	6
rCG34534	PP3111 protein	−2.313	−1.127	1
rCG60289.1	peroxisome proliferator activated receptor alpha	−2.829	−1.641	1
rCG21321.1	T-box 3	2.119	1.414	2
rCG32815	thymidine kinase 1	2.093	1.563	2
rCG48308	transducin-like enhancer of split 4, E(spl) homolog (drosophila)	2.345	1.217	3
rCG61469.1	twist gene homolog 1 (drosophila)	−1.007	2.001	7
rCG58097	zinc finger and BTB domain containing 16	−2.002	−4.239	6
Protein metabolism and modification				
rCG29689	alpha-2-macroglobulin	−3.486	1.283	1
rCG49423	UDP-Gal:betaGlcNAc beta 1,4-galactosyltransferase, polypeptide 6	2.069	1.638	2
rCG31859	caspase 12	1.530	−1.404	4
rCG60712.1	cell division cycle 2 homolog A (*S. pombe*)	2.083	−1.165	3
rCG56540	camello-like 3	2.019	1.137	3
rCG23512	crystallin, lamda 1	3.750	1.254	3
rCG46116.1	cathepsin E	−2.167	−1.805	6
rCG41001	cytochrome P450, subfamily 51	1.915	2.016	2
rCG51244	dipeptidase 1 (renal)	−2.080	−1.296	1
rCG48966	dual specificity phosphatase 6	1.885	−1.507	4
rCG40142	eukaryotic elongation factor-2 kinase	−1.947	−2.069	6
rCG28070	Eph receptor B6 (predicted)	−1.696	1.414	5
rCG42352.1	guanine nucleotide binding protein-like 3 (nucleolar)	1.992	2.686	2

Table 2. Continued

Gene ID	Gene name	Fold (STZ/N)[b]	Fold (EPS/N)[b]	Cluster
rCG57758	G protein-coupled receptor kinase 5	−1.164	−2.579	6
rCG44446	granzyme K	3.553	2.181	9
rCG53902.1	heterogeneous nuclear ribonucleoprotein methyltransferase-like 3 (*S. cerevisiae*)	−2.662	1.072	1
rCG21815	heat shock 27 kDa protein 1	4.727	2.081	9
rCG40557	integrin linked kinase	−2.281	−1.122	1
rCG25653	laminin receptor 1 (67 kD, ribosomal protein SA)	1.561	−1.325	4
rCG31028	matrix metalloproteinase 23	−2.517	−1.770	1
rCG56310	N-acetyltransferase 8 (camello like)	2.023	1.511	2
rCG23753	neuraminidase 2	5.567	1.236	9
rCG49547	protein phosphatase 2 (formerly 2A), regulatory subunit B (PR 52), beta isoform	2.448	1.757	2
rCG50988	protein kinase, AMP-activated, alpha 1 catalytic subunit	2.329	2.830	2
rCG61648.1	protein kinase C, epsilon	1.313	−1.956	4
rCG33834	protease, serine, 21	2.137	1.524	2
rCG20866	similar to serine proteinase inhibitor A11 gene (SERPINA11)	−2.123	−1.045	1
rCG51023	ribosomal protein L37	−3.255	−1.084	1
rCG44964.1	ribosomal protein S6 kinase polypeptide 2	1.274	−1.851	4
rCG56879	serine (or cysteine) peptidase inhibitor, clade A (alpha-1 antipeptidase, antitrypsin), member 7	1.947	−1.684	4
rCG57812	serine/threonine kinase 2	−2.024	−1.170	1
rCG37468.1	tribbles homolog 3 (Drosophila)	1.451	−1.529	4
rCG58615	ubiquitin D	3.096	−1.085	3
rCG48834	ubiquitin-conjugating enzyme E2N	−2.700	−1.204	1
Signal transduction				
rCG29689	alpha-2-macroglobulin	−3.486	1.283	1
rCG47519	annexin A1	−2.291	−1.844	6
rCG49353	adenomatosis polyposis coli	1.668	−1.429	4
rCG46238	B-cell translocation gene 2, anti-proliferative	2.512	1.469	2
rCG35264	cask-interacting protein 1	−1.718	1.535	5
rCG28162	caveolin 2	−4.809	−1.273	8
rCG28162	caveolin 2	−4.395	−1.442	8
rCG34044	chemokine (C-C motif) ligand 3	1.821	−1.287	4
rCG54820	cadherin 17	−2.165	−2.872	6
rCG53616.1	CEA-related cell adhesion molecule 10	2.225	1.262	3
rCG25343	cadherin EGF LAG seven-pass G-type receptor 3	1.977	2.013	2
rCG55586.1	chemokine orphan receptor 1	−2.035	−1.368	1
rCG45317	cAMP responsive element modulator	−2.234	−1.341	1
rCG60405	chemokine (C-X-C motif) ligand 1	7.167	2.510	9
rCG43636	down syndrome critical region gene 1-like 1	2.011	−1.804	4
rCG49298	diphtheria toxin receptor	1.864	−1.935	4
rCG48966	dual specificity phosphatase 6	1.885	−1.507	4
rCG31607	endothelial differentiation, sphingolipid G-protein-coupled receptor, 5	−2.124	−1.548	1
rCG40142	eukaryotic elongation factor-2 kinase	−1.947	−2.069	6
rCG28070	Eph receptor B6 (predicted)	−1.696	1.414	5
rCG28808	fatty acid binding protein 2, intestinal	−1.613	−2.066	6
rCG21961	fatty acid binding protein 7, brain	−3.342	−2.079	8
rCG20641.1	fibulin 5	−3.444	−1.985	8
rCG46303	Fc receptor, IgG, low affinity IIb	2.155	1.166	3
rCG54320.1	fibroblast growth factor 21	−3.413	−2.176	8
rCG44062.1	HNF-3/forkhead homolog-1	5.272	1.541	9
rCG31029	gap junction membrane channel protein alpha 4	−2.385	−1.066	1
rCG42352.1	guanine nucleotide binding protein-like 3 (nucleolar)	1.992	2.686	2
rCG57758	G protein-coupled receptor kinase 5	−1.164	−2.579	6

Table 2. Continued

Gene ID	Gene name	Fold (STZ/N)[b]	Fold (EPS/N)[b]	Cluster
rCG24716	homer homolog 2 (Drosophila)	2.085	1.485	2
rCG48929	insulin-like growth factor 1	−2.830	−1.158	1
rCG24493	insulin-like growth factor binding protein 1	4.507	1.540	9
rCG23864	insulin-like growth factor binding protein 2	8.196	−2.371	3
rCG41634	interleukin 7	1.274	2.760	7
rCG40557	integrin linked kinase	−2.281	−1.122	1
rCG60295.1	inhibin beta C	−2.949	−1.265	1
rCG59891	inhibin beta E	−3.496	1.129	1
rCG50886.1	integrin beta 1	1.134	2.422	7
rCG53510.1	v-jun sarcoma virus 17 oncogene homolog (avian)	3.328	1.106	3
rCG30109	killer cell lectin-like receptor, subfamily D, member 1	2.104	1.637	2
rCG30255	Kirsten rat sarcoma viral oncogene homologue 2 (active)	−1.183	1.723	5
rCG61851.1	leucine rich repeat protein 3, neuronal	−1.817	−2.168	6
rCG48866	lumican	2.494	2.897	2
rCG51981	membrane-associated guanylate kinase-related (MAGI-3)	2.953	−1.090	3
rCG47320	multiple inositol polyphosphate histidine phosphatase 1	−2.952	−1.386	1
rCG35147	neurofibromatosis 1	1.068	−1.892	4
rCG43164	neuregulin 1	3.952	1.189	3
rCG50933	neuropilin 1	−4.243	−1.013	1
rCG29761	neurotrophin 3	1.632	2.331	7
rCG21538	purinergic receptor P2X, ligand-gated ion channel, 7	−5.551	−3.666	8
rCG53397	phosphodiesterase 4B	−2.520	−1.952	6
rCG53524.1	ER transmembrane protein Dri 42	−2.720	−1.234	1
rCG60289.1	peroxisome proliferator activated receptor alpha	−2.829	−1.641	1
rCG61648.1	protein kinase C, epsilon	1.313	−1.956	4
rCG28308	pleiotrophin	−3.353	−2.079	8
rCG44964.1	ribosomal protein S6 kinase polypeptide 2	1.274	−1.851	4
rCG62481	S100 calcium binding protein A9 (calgranulin B)	1.968	2.044	2
rCG56456	semaphorin 4f	−2.206	−1.588	1
rCG26600	solute carrier family 1 (glial high affinity glutamate transporter), member 2	2.133	−1.288	4
rCG35087	suppressor of cytokine signaling 3	4.140	1.838	9
rCG59982	somatostatin receptor 3	2.427	2.856	2
rCG38477.1	stathmin-like 3	5.059	2.344	9
rCG37468.1	tribbles homolog 3 (Drosophila)	1.451	−1.529	4
rCG28134	wingless-related MMTV integration site 2	2.145	1.218	3
Transport				
rCG52271	ATP-binding cassette, sub-family G (WHITE), member 2	−2.466	1.213	1
rCG61966	ATP-binding cassette, sub-family G (WHITE), member 5	−1.568	−2.066	6
rCG62170	ATP-binding cassette, sub-family G (WHITE), member 8	−1.119	−2.228	6
rCG58473	apolipoprotein A-IV	−3.046	−1.035	1
rCG58386	apolipoprotein A-V	−2.004	−1.423	1
rCG28162	caveolin 2	−4.809	−1.273	8
rCG28162	caveolin 2	−4.395	−1.442	8
rCG28808	fatty acid binding protein 2, intestinal	−1.613	−2.066	6
rCG21961	fatty acid binding protein 7, brain	−3.342	−2.079	8
rCG58431	FXYD domain-containing ion transport regulator 2	2.751	1.336	3
rCG42352.1	guanine nucleotide binding protein-like 3 (nucleolar)	1.992	2.686	2
rCG23900	potassium inwardly-rectifying channel, subfamily J, member 13	−1.135	1.811	7
rCG53028	myxovirus (influenza virus) resistance 2	−1.634	1.372	5
rCG21538	purinergic receptor P2X, ligand-gated ion channel, 7	−5.551	−3.666	8
rCG36423	probasin	−10.559	−1.872	8

Table 2. Continued

Gene ID	Gene name	Fold (STZ/N)[b]	Fold (EPS/N)[b]	Cluster
rCG21954	prosaposin	−2.455	−1.057	1
rCG62828.1	rhesus blood group-associated B glycoprotein	2.367	1.304	3
rCG44022	Rsec5 protein	−2.123	−1.095	1
rCG41238	solute carrier family 14 (urea transporter), member 2	2.172	1.389	2
rCG26600	solute carrier family 1 (glial high affinity glutamate transporter), member 2	2.133	−1.288	4
rCG47649.1	solute carrier family 22 (organic anion transporter), member 8	−1.871	1.313	5
rCG53219	solute carrier family 25 (mitochondrial carrier, brain), member 14	−2.104	−1.504	1
rCG45392	solute carrier family 25 (mitochondrial carrier, phosphate carrier), member 25	−4.257	−1.023	1
rCG30703.1	solute carrier family 2, member 5	−1.266	2.856	7
rCG47505	integral membrane transport protein UST4r	1.754	−1.524	4

[a]Microarray analysis was performed as described in Material & Methods.
[b]N group rats were compared to STZ and EPS group rats. Animal groups are described in Materials and Methods. Results were expressed as fold increase (+) or decrease (−) in the gene expression. Data is shown as signal $\log_2$ ratio to N group.

most of these six genes increased again by EPS treatment.

2. Carbohydrate Metabolism

About 70% of genes in carbohydrate metabolism were down-regulated in response to STZ treatment. Among these, several major genes related to glycolysis were observed. These included genes encoding lactate dehydrogenase A and pyruvate dehydrogenase phosphatase isoenzyme 2. The major cause of fasting hyperglycemia in both type 1 and type 2 diabetes mellitus is decreased glycolysis and increased gluconeogenesis in liver. Pyruvate dehydrogenase phosphatase is an Mg^{2+}-dependent and Ca^{2+}-stimulated protein serine phosphatase that catalyzes the dephosphorylation and concomitant reactivation of the mitochondrial pyruvate dehydrogenase multienzyme complex. In our investigation, STZ treatment decreased the expression of pyruvate dehydrogenase phosphatase isoenzyme 2 (−1.821 fold), and increased again to around normal level (1.183-fold) by EPS administration.

STZ treatment also decreased the gene expression of lactate dehydrogenase A, suggesting an enhanced role for glycolysis in energy production. Lactate dehydrogenase is an oxidoreductase that catalyzes the conversion of lactate to pyruvate. Dhahbi et al. [29] reported that STZ-induced diabetes increased expression of the gene encoding lactate dehydrogenase 1. However, El-Demerdash et al. [33] reported that lactate dehydrogenase activity was significantly increased in plasma and testes of alloxan-induced diabetic rats, while the activities were decreased in liver compared with the control group. In this study, EPS therapy increased these glycolysis-related genes, suggesting that the cause of decreased plasma glucose level in EPS-treated diabetic rat results, at least partially, from stimulation of glycolysis.

3. Immunity and Defense

Among the genes associated immunity and defense, about 64% of genes were up-regulated in response to STZ treatment, which included chemokine (C-X-C motif) ligand 1, granzyme K, heat shock 27 kDa protein 1, and carboxylesterase 2 (Table 2 and Fig. 1). Carboxylesterases are a family of serine-dependent esterases involved in the metabolism of endogenous lipids and drugs by hydrolyzing ester groups of drugs and toxins [34-37]. Xu et al. [38] reported that human carboxylesterase 2 is commonly expressed in tumor tissue and is correlated with activation of irinotecan chemotherapy for solid tumors. In this study, the expression of carboxylesterase 2 was increased in STZ-induced diabetic rat liver and was decreased again by EPS treatment.

4. Lipid, Fatty Acid, and Steroid Metabolism

The expressions of many gene-associated lipid, fatty acid, and steroid metabolism were significantly changed in response to STZ treatment, which included cytochrome P450, family 26, subfamily A, polypeptide 1 and stearoyl-Coenzyme A desaturase 1 (Table 2 and Fig. 1). Stearoyl-CoA desaturase, the rate-limiting enzyme in monounsaturated fatty acid synthesis, has recently been shown to be the critical control point regulating hepatic lipogenesis and lipid oxidation [39]. Deficiency of stearoyl-CoA desaturase, although having no role in gluconeogenesis, powerfully induces fatty acid oxidation and weight loss despite increased food intake in rodents [40]. Activation of fatty acid oxidation has considerable clinical promise for the treatment of obesity, type 2 diabetes, steatohepatitis, and lipotoxic damage to the heart. The expression of stearoyl-CoA desaturase 1 was decreased to −6.945 fold in STZ-induced rat liver, and remarkably increased to 14.849 fold in EPS-treated diabetic rat liver. This result is consistent with those of previous studies showing that the activity and mRNA level of this enzyme are strongly inhibited in STZ-induced rat liver [41,42]. Dhahbi et al. [29] also reported that it was decreased to −14 fold in STZ-induced diabetic rat liver. The monounsaturated products are used as substrates for the synthesis of triglycerides, cholesterol esters, and membrane phospholipids. Inhibition of this enzyme alters membrane phospholipids composition, and this alteration is implicated in the pathology of diabetes.

STZ treatment also increased the gene expression of squalene epoxidase that catalyzes the first oxygenation step in sterol biosynthesis and is thought to be one of the rate-limiting enzymes in this pathway. This change would be expected to contribute to the increased cholesterol level observed in STZ-treated rats [43]. In this study, the expression of squalene epoxidase gene was slightly decreased by EPS therapy.

5. Signal Transduction

The expression of many gene-associated signal transductions was changed by STZ treatment and restored by EPS treatment (Table 2).

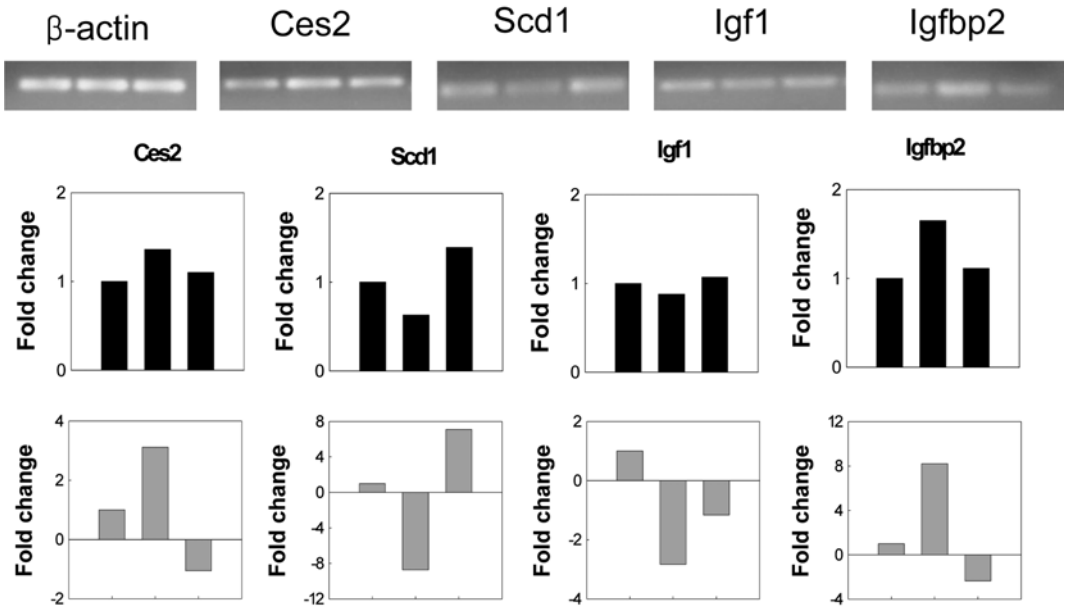

Fig. 3. Validation of the DNA chip data with RT-PCR. The expressions of four genes of interest were analyzed using DNA chip ( ) and RT-PCR ( ). The changes in the expression of the genes were similar in the direction and the magnitude between the two techniques.

The induction of insulin-like growth factor binding protein 2 found here is consistent with the results of previous reports, and extends published results regarding the level of this protein in the serum of STZ-induced diabetic rats [44,45]. Increased expression of this mRNA likely leads to decreased levels of bioavailable insulin-like growth factor 1, and to reduced rates of cell division and growth. The expression of insulin-like growth factor 1 also decreased in the liver of STZ-induced diabetic rats. These results are related to the fact that uncontrolled diabetes mellitus is characterized by poor growth and development in both humans and rodents. The abnormal expressions of theses genes were also rescued by EPS therapy.

To validate the microarray results, gene expression patterns of several genes of interest were confirmed by RT-PCR analysis. Gene expression trends of the four diabetes-specific genes (e.g. carboxylesterase 2, stearoyl-Coenzyme A desaturase 1, and insulin-like growth factor binding protein 2) are given in Fig. 3. RT-PCR confirmed gene expression trends to be similar to the microarray results.

CONCLUSION

To better distinguish the molecular genetic effects associated with its pathology in diabetic rat liver, we used oligonucleotide microarrays interrogating approximately 27,088 genes. Our findings provide novel insights into the changes in gene expression that may mediate aspects of diabetic pathophysiology, suggesting new potential targets for gene therapy and drug discovery. Our study is the first report showing that hypoglycemic polysaccharides directly signal in rat liver to regulate the expression of many metabolically important genes.

ACKNOWLEDGMENTS

This work was supported by Daegu University Research Grant 2008.

REFERENCES

1. E. Shmueli, C. O. Record and K. G. Alberti, *Baillieres. Clin. Endocrinol. Metab.*, **6**, 719 (1992).
2. R. Chatila and A. B. West, *Medicine (Baltimore)*, **75**, 327 (1996).
3. K. R. Feingold, M. H. Wiley, G. MacRae, A. H. Moser, S. R. Lear and M. D. Siperstein, *Diabetes*, **31**, 388 (1982).
4. S. V. McLennan, S. Heffernan, L. Wright, C. Rae, E. Fisher, D. K. Yue and J. R. Turtle, *Diabetes*, **40**, 344 (1991).
5. A. K. Saxena, P. Srivastava, R. K. Kale and N. Z. Baquer, *Biochem. Pharmacol.*, **45**, 539 (1993).
6. H. J. Hwang, S. W. Kim, Y. M. Baek, S. H. Lee, H. S. Hwang, S. G. Kumar, Md. A. Rahman and J. W. Yun, *Korean J. Chem. Eng.*, **25**, 308 (2008).
7. Y. Yamamoto, M. Nakajima, H. Yamazaki and T. Yokoi, *Life Sci.*, **70**, 471 (2001).
8. K. G. Tolman and J. Chandramouli, *Clin Liver Dis.*, **7**, 369 (2003).
9. A. S. Attele, Y. P. Zhou, J. T. Xie, J. A. Wu, L. Zhang, L. Dey, W. Pugh, P. A. Rue, K. S. Polonsky and C. S. Yuan, *Diabetes*, **51**, 1851 (2002).
10. J. T. Xie, H. H. Aung, J. A. Wu, A. S. Attele and C. S. Yuan, *Am. J. Chin. Med.*, **30**, 187 (2002).
11. J. T. Xie, Y. P. Zhou, L. Dey, A. S. Attele, J. A. Wu and M. Gu, *Phytomedicine*, **9**, 254 (2002).
12. M. Jung, M. Park, H. C. Lee, Y. H. Kang, E. S. Kang and S. K. Kim, *Curr. Med. Chem.*, **13**, 1203 (2006).
13. H. J. Hwang, S. W. Kim, J. M. Lim, J. H. Joo, H. O. Kim, H. M. Kim and J. W. Yun, *Life Sci.*, **76**, 3069 (2005).
14. S. W. Kim, H. J. Hwang, E. J. Cho, J. Y. Oh, Y. M. Baek, J. W. Choi and J. W. Yun, *J. Proteome Res.*, **5**, 2966 (2006).
15. S. W. Kim, H. J. Hwang, H. M. Kim, M. C. Lee, M. S. Lee, J. W.

Choi and J. W. Yun, *Proteomics*, **6**, 5291 (2006).
16. C. G. Fathman, L. Soares, S. M. Chan and P. J. Utz, *Nature*, **435**, 605 (2005).
17. V. S. Gomase, S. Tagore and K. V. Kale, *Curr Drug Metab*., **9**, 221 (2008).
18. R. García-Escudero and J. M. Paramio, *Mol. Carcinog*., **6**, Epub ahead of Print (2008).
19. J. P. Jakupciak, G. D. Dakubo, S. Maragh and R. L. Parr, *Curr. Opin. Mol. Ther.*, **8**, 500 (2006).
20. S. Iida, Y. Sato, A. Nakaya, Y. Shinohara, Y. Hayashi, A. Sawada, H. Nagata, N. Kaji, H. Kamiya, Y. Baba and H. Harashima, *Biol. Pharm. Bull.*, **29**, 2451 (2006).
21. I. Murtaza, G. Marra, R. Schlapbach, A. Patrignani, M. Kunzli, U. Wagner, J. Sabates and A. Dutt, *Biotechnol. Appl. Biochem.*, **45**, 29 (2006).
22. F. Allantaz, D. Chaussabel, J. Banchereau and V. Pascual, *Curr. Opin. Immunol*., **19**, 623 (2007).
23. K. Driouch, T. Landemaine, S. Sin, S. Wang and R. Lidereau, *Clin. Exp. Metastasis*, **24**, 575 (2007).
24. J. B. Welsh, P. P. Zarrinkar, L. M. Sapinoso, S. G. Kern, C. A. Behling, B. J. Monk, D. J. Lockhart, R. A. Burger and G. M. Hampton, *Proc. Natl. Acad. Sci. USA*, **98**, 1176 (2001).
25. T. R. Golub, D. K. Slonim, P. Tamayo, C. Huard, M. Gaasenbeek, J. P. Mesirov, H. Coller, M. L. Loh, J. R. Downing, M. A. Caligiuri, C. D. Bloomfield and E. S. Lander, *Science*, **286**, 531 (1999).
26. J. S. Hu, M. Durst, R. Kerb, V. Truong, J. T. Ma, E. Khurgin, D. Balaban, T. R. Gingeras and B. B. Hoffman, *Ann. NY Acad. Sci.*, **919**, 9 (2000).
27. A. Zisman, O. D. Peroni, E. D. Abel, M. D. Michael, F. Mauvais-Jarvis, B. B. Lowell, J. F. Wojtaszewski, M. F. Hirshman, A. Virkamaki, L. J. Goodyear, C. R. Kahn and B. B. Kahn, *Nat. Med.*, **6**, 924 (2000).
28. J. Wada, H. Zhang, Y. Tsuchiyama, K. Hiragushi, K. Hida, K. Shikata, Y. S. Kanwar and H. Makino, *Kidney Int.*, **59**, 1363 (2001).
29. J. M. Dhahbi, P. L. Mote, S. X. Cao and S. R. Spindler, *Diabetes Technol. Ther.*, **5**, 411 (2003).
30. K. Susztak, E. Bottinger, A. Novetsky, D. Liang, Y. Zhu, E. Ciccone, D. Wu, S. Dunn, P. McCue and K. Sharma, *Diabetes*, **53**, 784 (2004).
31. H. Mi, B. Lazareva-Ulitsky, R. Loo, A. Kejariwal, J. Vandergriff, S. Rabkin, N. Guo, A. Muruganujan, O. Doremieux, M. J. Campbell, H. Kitano and P. D. Thomas, *Nucleic Acids Res.*, **33**, D284 (2005).
32. Y. Ohtsuka and Y. Agishi, *Nippon Rinsho.*, **50**, 1631 (1992).
33. F. M. El-Demerdash, M. I. Yousef and N. I. El-Naga, *Toxicol.*, **43**, 57 (2005).
34. P. M. Potter, J. S. Wolverton, C. L. Morton, D. O. Whipple and M. K. Danks, *Cytometry*, **32**, 223 (1998).
35. W. Zhu, L. Song, H. Zhang, L. Matoney, E. Lecluyse and B. Yan, *Drug Metab. Dispos.*, **28**, 186 (2000).
36. T. Yamada, M. Hosokawa, T. Sotoh, I. Moroo, M. Takahashi and H. Akatsu, *Brain Res.*, **658**, 163 (1994).
37. T. Satoh and M. Hosokawa, *Annu. Rev. Pharmacol. Toxicol.*, **38**, 257 (1998).
38. G. Xu, W. Zhang, M. K. Ma and H. L. McLeod, *Clin. Cancer Res.*, **8**, 2605 (2002).
39. A. Dobrzyn and J. M. Ntambi, *Obes. Rev.*, **6**, 169 (2005).
40. D. W. Foster, *Ann. NY Acad. Sci.*, **1033**, 1 (2004).
41. M. Nishida, T. Sasaki, H. Terada and J. Kawada, *Experientia.*, **44**, 756 (1988).
42. K. M. Waters and J. M. Ntambi, *J. Biol. Chem.*, **269**, 27773 (1994).
43. B. Ramesh and K. V. Pugalendi, *Yale J. Biol. Med.*, **78**, 189 (2005).
44. G. T. Ooi, L. Y. Tseng and M. M. Rechler, *Biochem. Biophys. Res. Commun.*, **189**, 1031 (1992).
45. B. D. Rodgers, R. M. Bautista and C. S. Nicoll, *Proc. Soc. Exp. Biol. Med.*, **210**, 234 (1995).